Paper re-submitted to the Journal of Structural Engineering, ASCE in December 2012

Repair of Fire-exposed Preloaded Rectangular Concrete Columns by Post-compressed Steel Plates

Lu Wang[1], Ray Kai-Leung Su[2]

Abstract

This paper describes an experimental study of axially loaded, fire-exposed, rectangular reinforced concrete (RC) columns repaired with post-compressed steel plates. Seven RC columns with identical section dimensions and reinforcement details were fabricated and tested. Six of them were exposed to a four-hour fire load according to the ISO 834 Standard. After one month of cooling, five of the fire-exposed columns were installed with precambered steel plates which were then post-compressed by a method newly developed by the authors. All columns were tested under axial compression to determine their ultimate load capacity, deformation and ductility. The effects of steel plate thickness, initial precamber displacements and preloading level on the ultimate load capacity of repaired RC columns were investigated. The test results show that up to 72% of the original capacity of the axial load-carrying capacity of fire-exposed columns repaired with post-compressed steel plates can be restored. Furthermore, the repaired specimens show better ductility and post-peak deformability. An analytical model was adopted to predict the ultimate axial load capacity of fire-exposed columns repaired with post-compressed steel plates. Comparison of the theoretical and experimental results reveals that the analytical model can accurately predict the ultimate axial load capacity of the repaired columns.

Keywords Reinforced concrete columns, Fire, Post-compressed, Precambered Steel Plates, Repair, Analytical model

[1] PhD Candidate, Dept. of Civil Engineering, The Univ. of Hong Kong, Pokfulam Rd., Hong Kong, E-mail: wanglu@hku.hk

[2] Associate Professor, Dept. of Civil Engineering, The Univ. of Hong Kong, Pokfulam Rd., Hong Kong, corresponding author. E-mail: klsu@hkucc.hku.hk

Introduction

It is well known that fires cause great loss of life and property damage in the world. In 2011, public fire departments in the United States (US) responded to 1,389,500 fires, which caused about 3005 deaths, 17,500 injuries and property damage of 12 billion US dollars. In addition, 484,500 were structural fires, accounting for 35% of all fires, which increased by 0.5% compared to last year (Karter. 2012). Hence, to improve the safety of structures after fire exposure, there is a growing need to provide measures for post-fire repair of structural components.

When reinforced concrete (RC) columns acting as a primary load-bearing system in a building are exposed to a fire, it is more economical to repair the columns than to rebuild them to restore the original designed capacity. In the past two decades, many studies have been conducted to investigate the fire resistance of RC columns and their post-fire residual strength, stiffness and deformation (Bisby et al. 2004; Chen et al. 2009; Chowdhury et al. 2007; Han et al. 2009; Han et al. 2006; Kodur et al. 2006; 2009; Lie et al. 1996; Tao et al. 2011; Wu et al. 2007; Wu and Xu 2009; Xu and Wu 2009; Yaqub and Bailey 2011). Jau and Huang (2008) studied the fire resistance behavior of RC corner columns with 2-hour to 4-hour asymmetric fire loading under axial loading and biaxial bending. The relationship among the fire exposure time, steel ratio and thickness of cover was investigated. Kodur et al. (1998; 2003; 2004) and Raut and Kodur (2011) studied the fire resistance behavior of high strength concrete columns and high strength concrete-filled steel columns. A numerical model was proposed to evaluate the performance of high strength concrete columns exposed to fire. Many significant parameters were considered in this model, such as section dimensions, fiber reinforcement, column height, concrete strength and aggregate type. Han et al. (2001; 2002; 2003; 2004) and Han and Huo (2003) tested a large number of fire-exposed concrete-filled steel tubular columns. They developed a corresponding mathematical model for predicting the fire resistance and the fire protection thickness of the concrete-filled steel tubular columns.

Although extensive experimental and theoretical studies have been conducted to investigate the fire resistance of RC columns, only a few studies focused on repairing the fire-damaged RC columns. The

compressive strength of fire-exposed concrete-filled steel tubular columns repaired with fibre-reinforced polymer (FRP) wraps was investigated (Tao and Han 2007; Tao et al. 2007). The test results demonstrated that the FRP confinement can increase the axial load-carrying capacity and stiffness of fire-exposed columns, but the strength of fire-exposed columns was not fully restored due to the long fire exposure time (≥ 180 minutes). For circular columns, the axial load-carrying capacities of the FRP-strengthened short and slender columns can be restored, respectively, to 61.2% and 34.5% of the original designed capacity; for square columns, the axial load-carrying capacities of the FRP-strengthened short and slender columns can be enhanced, respectively, to 46.6% and 28.4% of the original designed capacity. Lin et al. (1995) adopted a recast concrete method to repair fire-damaged RC columns. The repair work involved removing surface layers of concrete cover, surface cleaning and patching using specially designed concrete. The test results showed that most repaired columns could recover their original capacity or develop a capacity even higher than those of unheated columns.

However, no matter whether an FRP wrap or recast concrete is used to repair fire-exposed RC columns, the effects of preexisting loads on stress-lagging between the concrete core and the new jacket have yet to be determined. Ersoy et al. (1993), Takeuti et al. (2008), Giménez et al. (2009) and Su and Wang (2012) experimentally studied the effects of pre-existing loads on the strengthening efficiency. Their test results demonstrated that the stress-lagging effects can significantly reduce the ultimate axial load capacity of strengthened columns. Meanwhile, Tao and Han (2007) noted that FRP composites were more effective in enhancing the load-carrying capacity of fire-damaged circular columns than were square ones. Wang and Su (2012a; 2012b) conducted experimental and theoretical studies on the performance of preloaded RC columns strengthened with precambered steel plates under eccentric compression loads. In this approach, precambered steel plates were bolted to the RC column. Because the plates were slightly longer than the clear height of the column, progressive tightening of the anchor bolts could generate a thrust on the beam supports by means of arching action. Their results proved that precambered steel plates could actively share the existing axial loads with the original column. Stress relief in the original concrete column and post-stress developed in the steel

plates can alleviate the stress-lagging and displacement incompatibility problems. Nonetheless, as an economical and simple strengthening method, steel jacketing that is executed by attaching steel plates or angles onto the concrete has not been thoroughly studied for repairing fire-damaged RC columns.

In this study, precambered steel plates together with the post-decompression method were employed to strengthen fire-exposed preloaded RC columns. An experimental study was conducted to investigate the axial strength, post-peak deformability, ductility and internal load distributions between the concrete and the steel plates of plate-strengthened RC columns. The effectiveness of this repair method on the fire-exposed RC columns was examined. Finally, an analytical model with the consideration of the stress lagging effects was presented to predict the ultimate axial load capacity of fire-exposed RC columns repaired with post-compressed steel plates.

Experimental program

Test specimens

Seven specimens, namely FSC1 to FSC7, were fabricated and tested. The RC details of all specimens were identical. The RC cross sections were 300 mm × 250 mm, and the clear height of column was 850 mm. Six high-yield deformed bars with diameter 12 mm (T12) were arranged as the vertical reinforcement, and the mild steel round bars with diameter 6 mm (R6) were adopted as the transverse reinforcement, which were applied throughout the height of the column with spacing 80 mm. All of the specimens had the same concrete cover of 40 mm. To prevent local failure during the load test, both ends of the specimens were slightly enlarged and properly reinforced, as shown in Fig. 1.

The design data of the specimens are summarized in Table 1. Specimen FSC1 was a control column with no repair measures and no fire load, while Specimen FSC2 was a control column exposed to fire without any repair measures. They were used to demonstrate the structural performance of an RC column and a fire-exposed RC column prior to repair. The rest of the specimens were repaired by precambered steel plates with a thickness (t_p) of either 6 mm or 8 mm. The precamber at the middle height (δ) of columns (as shown in Figure 1) varied from 6 mm to 14 mm. All of the repaired columns

were subjected to a preloading level (P_{pl}) before flattening the precambered steel plates, which ranged from 0.21 to 0.27 of the ultimate axial load capacities of Specimen FSC1.

Material properties

The concrete has an aggregate-to-cement ratio of 4.10 and a water-to-cement ratio of 0.45 by weight. The mix incorporated 10 mm coarse aggregates, and the slump value was approximately 65 mm. For each specimen, four 150 mm × 150 mm × 150 mm concrete cubes and four Ø150 mm × 300 mm cylinders were cast, and compressive tests were performed to obtain the compressive strengths on the 28th day and the fire test day, as shown in Table 1.

Two types of high-yield deformed bars and two types of mild steel round bars were used in this study. Three 500-mm-long samples were taken from each type of reinforcement. Tensile tests were conducted to obtain the yield strength and Young's modulus of these samples. To determine the material properties of the steel plates, six 500 mm × 50 mm strips were taken from 6-mm-thick and 8-mm-thick steel plates for tensile tests. The material properties of the steel reinforcements and steel plates are summarized in Table 2.

Large-scale furnace and fire exposure

A large-scale furnace was built for full-scale fire tests on column, wall and floor elements at the Fire Laboratory of RED Fire and Facade Consultants Limited in Hong Kong, as shown in Fig. 2(a). The heat was provided by eight gas burners, with four burners on each side. The temperature of the concrete was monitored by K-type thermocouples that were located at various cross sections, as shown in Fig. 3. The column was exposed to fire following the ISO834 standard temperature-time curve (ISO 1975) for four hours, as plotted in Fig. 4.

$$T = 345\log_{10}(8t + 1) + T_0 \quad (1)$$

where T is the fire temperature (°C), t is the time in minutes and T_0 is the environmental temperature.

Setup for the axial compression test

The compression test was conducted at the Structural Laboratory of South China University of Technology. Loading was applied by a 15,000 kN hydraulic actuator. The upper head of the specimen was connected to a hydraulic jack, and the lower end of the specimen was connected to the strong floor, as shown in Fig. 2(b). All the plate-strengthened RC columns were subjected to preloading P_{pl} = 640 kN (which is about 50% of the axial load capacity of the fire control specimen) before strengthening, except Specimen FSC4 which adopted preloading P_{pl} = 830 kN. For plate-strengthened specimens, the axial load was applied under force control with a loading rate at 2 kN per second. After tightening the bolts and flattening the precambered plates, the applied load was changed to displacement control with a displacement rate of 0.008 mm per second. The test was terminated when the post-peak load reached 75% of the peak load.

Instrumentation

To measure the axial shortening of the columns, two linear variable displacement transducers (LVDTs) with a stroke of 30 mm were set symmetrically at opposite sides of the column. In each specimen, the strains in the steel plates were measured using electrical resistance linear strain gauges (TML Type FLA-5-11-3L, Tokyo Sokki Kenkyujo Co., Ltd.). Sixteen strain gauges were attached to the steel plates at four different sections along the height. The strains measured were then used to identify the failure mode and to investigate the axial load distributions in the specimens. The arrangement of LVDTs and strain gauges are depicted in Fig. 5.

Test procedure

The specimen was installed vertically in the furnace approximately one month after concrete casting. The fire procedure was under time control. After the specimen had been forced-air cooled to room temperature, the specimen was taken out of the furnace and stored in the laboratory for one month to ensure that the residual strength of the concrete would be minimized at the time of the axial load tests. Fig. 6 shows the cracks and spalls of the concrete after the fire test. To avoid local buckling of steel

plates, the cement mortar was used to repair the spalled concrete before installing the steel plates, as shown in Fig.7(a).

To control the initial precamber of the steel plates, two stainless steel rods with a diameter equal to the initial precamber were inserted and fixed between the concrete and steel plates at the middle height of the column. The bolts at both ends of the column were then tightened to generate the designed initial precamber profile. The gaps between the steel angles and the concrete at the bottom and top of the steel plates were filled with an injection plaster, forming a layer of bedding between the steel angles and the concrete, as shown in Fig. 7(b). The injection plaster was composed of plaster, potassium sulfate and water with a proportion of 37.5 : 1 : 15, by weight.

When the applied compression reached the preloading level, the post-stress procedure (Su and Wang 2012) was adopted to avoid warping or buckling of steel plates during the decompression of the RC column by flattening the precambered steel plates. Fig. 8(a) shows the post-stress procedure in detail, which can be divided into the following steps: Steps (i & ii), bolts at the mid-height are tightened, thus, the buckling mode of the precambered plates is changed to higher modes; Step (iii), the plates are flattened by tightening the other bolts; and in Steps (iv & v), to achieve a more evenly distributed internal stress in the plates, all the bolts are slightly loosened and re-fastened again. Fig. 8(b) and (c) show the post-stress procedure from Step (i) to Step (iii) and the strengthening details of Specimen FSC6, respectively.

Test results and evaluation

Concrete temperature distribution

Figs. 9(a) and 9(b) show the concrete temperature at various depths of the mid-height cross section (B-B). As shown in Fig. 9(a), after exposure to the ISO-834 standard fire for four hours, the concrete temperature 15 mm from the surface reached 955 °C, which was 77.5% and 143.0% greater than the concrete temperature at 70 mm (538 °C) and 125 mm (393 °C) from surface, respectively. As shown

191 in Fig. 9(b), after exposure to the fire for four hours, the concrete temperature at 50 mm from surface
192 was 622 °C, which was 27.5% greater than the concrete temperature at 100 mm (487 °C) from surface.
193 Figs. 9(c) and 9(d) show the concrete temperature at various heights for the same distance from the
194 concrete surface. As shown in Fig. 9(c), after exposure to the fire for four hours, the concrete
195 temperatures were 477 °C, 513 °C and 444 °C at Sections A-A, B-B and C-C, respectively. As shown
196 in Fig. 9(d), after exposure to the fire for four hours, the concrete temperatures were 417 °C, 471 °C
197 and 412 °C at Sections A-A, B-B and C-C, respectively. The fire test results show that smaller
198 distances from the concrete surface can lead to higher concrete temperatures, while the concrete
199 temperature at the same concrete depth was evenly distributed along the column height.
200
201 ***Strength analysis***
202 Compared with the post-fire control column (FSC2), the repaired specimens show various degrees of
203 strengthening from 18.9% to 74.0%, which are summarized in Table 3. The ultimate load capacities of
204 Specimens FSC3, FSC4, FSC5, FSC6 and FSC7 were increased by 74.0%, 31.7%, 18.9%, 52.3% and
205 68.2%, respectively. Compared with the ultimate load capacity of the control column (FSC1), the
206 ultimate load capacities of Specimens FSC3, FSC4, FSC5, FSC6 and FSC7 are restored up to 72.2%,
207 54.7%, 49.3%, 63.2% and 69.8%, respectively.
208 Fig. 10(a) shows the effects of fire on the ultimate load capacity of RC columns. Compared with the
209 control column FSC1 (P_{exp}=3085 kN), the ultimate load capacity of Specimen FSC2 decreased by
210 58.5%. Fig. 10(b) shows the effects of the plate thickness (t_p) on the ultimate load capacity (P_{exp})
211 under the same preloading level and initial precamber. Compared with Specimen FSC2 (t_p = 0 mm),
212 the ultimate load capacities of Specimens FSC3 (t_p = 8 mm) and FSC6 (t_p = 6 mm) increased by
213 74.0% and 52.3%, respectively. Fig. 10(c) shows the effects of the initial precamber (δ) on the
214 ultimate load capacity. The ultimate load capacity of Specimen FSC7 with δ = 14 mm was 2153 kN,
215 which was 41.5% and 10.4% larger than the ultimate load capacities of Specimens FSC5 (δ = 6 mm)
216 and FSC6 (δ = 10 mm), respectively. Because a larger initial precamber could generate a greater post-

compressive force in the steel plates, a greater preloading in the original RC column could therefore be transferred to the steel plates. The reduction in the strain incompatibility between the steel plates and concrete enhanced the ultimate load capacity of FSC7. Fig. 10(d) shows the effects of preloading level (P_{pl}) on the ultimate load capacity (P_{exp}). Compared with Specimen FSC6 (P_{pl} = 640 kN), the ultimate load capacity of Specimen FSC4 (P_{pl} = 830 kN) decreased by 15.7%. It is because the higher preloading in Specimen FSC4 leading to larger locked in axial stress in the concrete. Hence, the steel plate strength utilisation coefficient (γ) defined in Equation (11) is lower than that of Specimen FSC6. The results clearly demonstrate that the use of thicker plates or increasing the initial precamber of plates can achieve a significantly higher ultimate load capacity.

Crack patterns and failure modes

The concrete crack patterns of all of the specimens were quite similar after load tests. The initial concrete cracks usually occurred at the mid-height of the columns and then propagated in the vertical direction. With an increasing applied load, the major cracks were extended, and the concrete was spalled, as shown in Fig. 11. Judging from the readings of the strain gauges attached to the steel plates, the failure modes of specimens were identified. To avoid plate local buckling, the bolt spacing of 180 mm was adopted so that the critical buckling stress was larger than the yield stress of steel plates. According to the strain readings, once the concrete crushing occurred, the steel plates reached their yield strength rapidly because the resistance force originally provided by the concrete was changed to that provided by the steel plates.

Deformation and Ductility

The deformability factor (λ), which is defined in Equation (2) by De Luca et al. (2011), was adopted to evaluate the deformation performance of the repaired columns.

$$\lambda = \Delta_f / \Delta_u \tag{2}$$

in which Δ_u is the axial shortening at the ultimate load and Δ_f is the axial shortening at the failure load, which is equal to 75% of the ultimate load. The deformability factors of specimens were calculated, and the results, ranging from 1.12 (Specimen FSC1) to 1.73 (Specimen FSC3), are summarized in Table 3. Compared with the control column, the deformability factor of the post-fire control column (FSC2) was 1.19, an increase of only 6.3%. However, the deformability factors of Specimens FSC3, FSC4, FSC5, FSC6 and FSC7 were increased by 54.5%, 39.3%, 19.6%, 38.4% and 34.8%, respectively. Thus, the plate thickness plays an important role in increasing the deformability of the repaired columns.

The displacement ductility factor (η) is introduced to evaluate the ductility performance of the repaired columns, which is defined as the ratio of the axial shortening at the ultimate load (Δ_u) to the notional yield displacement (Δ_y) (Su et al. 2010), thus

$$\eta = \Delta_u / \Delta_y \tag{3}$$

As shown in Table 3, the displacement ductility factors range from 1.09 (for Specimen FSC1) to 2.21 (for Specimen FSC3). Compared with the control column, the displacement ductility factor of the post-fire control column (FSC2) was 1.42, increased by 30.3%. Compared with Specimen FSC5 (δ = 6 mm), the displacement ductility factors of Specimens FSC6 (δ = 10 mm) and FSC7 (δ = 14 mm) were increased by 20.8% and 21.4%, respectively. The difference of the displacement ductility factors between Specimens FSC6 and FSC7 was only 0.6%. It is because the plate strength utilization coefficients (γ) of Specimens FSC6 (γ = 0.90) and FSC7 (γ = 0.99) were quite similar, while their coefficients were much higher than that of Specimen FSC5 (γ = 0.68). Using thicker plates (t_p = 8 mm) for Specimen FSC3 instead of thinner plates (t_p = 6 mm) for Specimen FSC6, the displacement ductility factor of FSC3 was increased by 5.7 %. Compared with Specimen FSC6 (P_{pl} = 640 kN), the displacement ductility factor of Specimen FSC4 (P_{pl} = 830 kN) was slightly increased by 1.0%. Hence, using a larger initial precamber (which led to higher plate strength utilization) and thicker steel plates could effectively improve the displacement ductility, while the effect of the preloading level on the displacement ductility was relatively small.

Distribution of axial forces between steel plates and concrete

The distribution of loads between the original RC column and the steel plates is a key issue in this study. Sixteen strain gauges were pasted at four different sections on the steel plates to evaluate this distribution, as shown in Fig. 5. The load distributions of strengthened columns FSC3, FSC4, FSC5, FSC6 and FSC7 at three different loading stages including (i) the preloading (after tightening the bolts), (ii) 75% of the peak load and (iii) the peak load are summarized in Table 4. These figures show that the axial load was almost uniformly distributed across the height of the plates. For Specimen FSC3, the largest variation in the axial load distribution was only 55 kN when the load reached 75% of the peak load. For Specimen FSC4, the largest axial load variation was 84 kN, which occurred between Section 1 and Section 3 at the peak loading stage. For Specimens FSC5 and FSC6, the largest axial load variations were 77 kN and 67 kN, respectively. For Specimen FSC7, the largest variation was 89 kN, which occurred between Section 1 and Section 2 at 75% of the ultimate load. These results suggest that the proposed post-stress procedure is an effective means to achieve axial load sharing between the original column and the additional steel plates.

Analytical model

Residual strength of concrete and steel bars

It is well known that compressive strength of concrete would vary according to the fire exposure time. The residual strength of concrete (f_{cr}') may be estimated by Equation (4) (Tan and Yao, 2003).

$$f_{cr}^{'} = \beta_c \times f_c^{'} \tag{4}$$

where f_c' is the cylinder compressive strength of concrete, and β_c is the strength reduction factor for concrete, which can be determined by Equation (5) (Dotreppe et al., 1997).

$$\beta_c = \frac{\mu}{\sqrt{1+(0.3A_c^{-0.5}t_{ISO})^{A_c^{-0.25}}}} \tag{5}$$

in which A_c is the cross sectional area of RC column in m^2, t_{ISO} is the ISO 834 fire exposure time in hours, and μ is the factor to account for spalling of concrete, which can be obtained by Equation (6).

$$\mu = \begin{cases} 1 - 0.3t_{ISO} & (t_{ISO} \le 0.5 \text{ hour}) \\ 0.85 & (t_{ISO} > 0.5 \text{ hour}) \end{cases} \quad (6)$$

The residual strength of steel bars (f_{sy}') can be determined by Equation (7) (Lie, 1992).

$$f_{sy}^{'} = \begin{cases} f_{sy}[1.0 + \dfrac{T}{900\ln(\dfrac{T}{1750})}] & (0 < T \le 600^{o}\text{C}) \\ f_{sy}(\dfrac{340 - 0.34T}{T - 240}) & (600^{o}\text{C} < T < 1000^{o}\text{C}) \end{cases} \quad (7)$$

where f_{sy} is the yield strength of steel reinforcement, and T is the temperature of steel bar.

Ultimate load capacity of repaired columns

Su and Wang (2012) proposed a theoretical model to predict the ultimate axial load capacity of RC column strengthened with post-compressed steel plates. The theory of this method is similar to the principle of pre-stressed concrete. The amount of post-compressed plate forces induced is controlled by the initial precamber of the precambered plates. The ultimate axial load capacity (P_{pre}) of the plate-repaired column is expressed as

$$P_{pre} = 0.85A_c f_{cr}^{'} + A_s f_{sy}^{'} + 2\gamma A_p f_{py} \quad (8)$$

where A_s and A_p are the cross-sectional area of longitudinal reinforcement and steel plates respectively, f_{py} is the yield strength of steel plates, and γ is the plate strength utilisation coefficient, which can be estimated as

$$\gamma = \begin{cases} \dfrac{E_p(\varepsilon_{co} - \varepsilon_{c,ps})}{f_{py}} & (\varepsilon_{co} - \varepsilon_{c,ps} < \varepsilon_{py}) \\ 1 & (\varepsilon_{co} - \varepsilon_{c,ps} \ge \varepsilon_{py}) \end{cases} \quad (9)$$

where E_p is Young's moduli of steel plates, ε_{co} is the concrete compressive strain corresponding to $f_c^{'}$, ε_{py} is the yield strain of the steel plates, and $\varepsilon_{c,ps}$ is the concrete strain at the post-stressing stage, which can be determined from Equation (10),

313 $$\varepsilon_{c,ps} = \frac{\varepsilon_{c0}(2A_c f_c^{'} + E_s A_s \varepsilon_{c0} - \sqrt{4A_c f_c^{'}(A_c f_c^{'} + E_s A_s \varepsilon_{c0} + 2E_p A_p \varepsilon_{p,ps} - P_{pl}) + E_s^2 A_s^2 \varepsilon_{c0}^2})}{2A_c f_c^{'}} \quad (10)$$

314 where E_s is Young's moduli of longitudinal reinforcement, P_{pl} is the preloading, and $\varepsilon_{p,ps}$ is the strain
315 of steel plate when the precambered plate was flattened, which can be determined by Equation (11),

316 $$\varepsilon_{p,ps} = [(\frac{(\pi\delta)^2}{4L_{rc,pl}})(\frac{2K_p K_{rc,pl}}{2K_p + K_{rc,pl}})] / (E_p A_p) \quad (11)$$

317 where $L_{rc,pl}$ is the clear height of the RC column under preloading (P_{pl}), δ is the initial precamber at the
318 mid-height of the plate, and K_p and $K_{rc,pl}$ are the axial stiffnesses of a steel plate and RC column
319 respectively, which can be determined from Equation (12) and Equation (13), respectively.

320 $$K_{rc,pl} = \frac{E_c A_c}{L_{rc,pl}} \quad (12)$$

321 $$K_p = \frac{E_p A_p}{L_p} \quad (13)$$

322 where L_p is the length of the steel plate.

323

324 ***Fire resistance requirements for repaired columns***

325 Due to the use of steel plates, fire protection of the structural steel should be a concern. A common fire
326 protection for repaired columns is to box in using gypsum wallboard, as shown in Fig.12. The fire
327 resistance of the repaired columns protected by gypsum wallboard can be determined by Equation (14)
328 (ASCE/SEI/SFPE 2007).

329 $$R = 1.6(\frac{h\frac{W^{'}}{D}}{2})^{0.75} \quad (14)$$

330 where R is the fire resistance in minutes, h is the thickness of gypsum wallboard in mm, D is the
331 heated perimeter in mm, and $W^{'}$ is the weight of steel and gypsum wallboard protection per foot length
332 in kg/m, which can be determined by Equation (15) (ASCE/SEI/SFPE 2007).

333 $$W^{'} = W + 0.0008hD \quad (15)$$

where W is the average weight of the steel in kg/m.

Comparison between the predicted and experimental results

Using Equations (8) to (13), the ultimate axial load capacity of repaired columns was evaluated. The predicted axial load capacity (P_{pre}) of the specimens is listed in Table 3. It is noted that the strain of concrete corresponding to the peak load (ε_{co}) was taken as 0.002 in the calculation. Comparing the theoretical and experimental axial load capacities reveals that the analytical model is generally able to conservatively estimate the axial load capacity of fire-exposed RC columns repaired with post-compressed steel plates with an average underestimation of 12%.

Conclusions

This paper presents a study on the axial strengthening of fire-exposed RC columns using post-compressed steel plates under axial compression loading. The main findings of this study can be summarized as follows:

(1) The axial load-carry capacity of RC columns with a cross section of 300 mm × 250 mm can decrease drastically when the columns are subjected to a four-hour fire load. The concrete temperature increases sharply in the concrete cover near the concrete surface.

(2) Compared with the test results of Tao and Han (2007), the proposed repairing method by post-compressed steel plates is more effective in restoring the axial load-carrying capacity of fire-exposed concrete rectangular columns than FRP wraps.

(3) Test results show that the axial load-carrying capacity of four-hour fire-exposed columns repaired with post-compressed steel plates can restore up to 72% of the original ultimate load level. If thicker steel plates were used, the strength of these columns could increase further.

(4) The experimental results show that post-compressed precambered steel plates can share the existing axial load in the original column. Stress-lagging effects can be alleviated by controlling the initial precambered profile of the steel plates.

(5) External steel plates can considerably enhance the axial strength and the deformation capacity of plate-strengthened columns under axial compression loading.

(6) Thicker steel plates and a larger initial precamber can enhance the ultimate load capacity of columns. The use of a larger plate thickness can also improve the axial deformation capacity of columns significantly.

(7) An analytical model to predict the ultimate axial load capacity of fire-exposed columns repaired with post-compressed steel plates was described. The comparison between the theoretical and experimental results indicates that the model adopted can accurately predict the ultimate axial load capacity of plate-repaired columns.

ACKNOWLEDGMENTS

The research described here was supported by the Research Grants Council of the Hong Kong SAR (Project No. HKU7166/08E) and The University of Hong Kong through Small Project Funding 2010-2011.

REFERENCES

ASCE/SEI/SFPE 29-05 (2007) Standard calculation method for structural fire protection, American Society of Civil Engineers, Reston, VA.

Bisby, L. A., Kodur, V. K. R., and Green, M. F. (2004). ‘‘Numerical parametric studies on the fire endurance of fibre-reinforced-polymer-confined concrete columns.’’ *Canadian Journal of Civil Engineering*, 31(6), 1090–1100.

Chen, Y. H., Chang, Y. F., Yao, G. C., and Sheu, M. S. (2009). “Experimental research on post-fire behaviour of reinforced concrete columns.” *Fire Safety Journal*, 44(5), 741–748.

Chowdhury, E. U., Bisby, L. A., Green, M. F., and Kodur, V. K. R. (2007). “Investigation of insulated FRP-wrapped reinforced concrete columns in fire.” *Fire Safety Journal*, 42(6), 452–460.

De Luca, A., Nardone, F., Matta, F., Nanni, A., Liqnola, G., and Prota, A. (2011). “Structural evaluation of full-scale FRP-confined reinforced concrete columns.” *Journal of Composites for Construction*, 15(1), 112-123.

Dotreppe, J. C., Franssen, J. M., Bruls, A., Vandevelde, P., Minne, R., Van Nieuwenburg, D., and Lambotte, H. (1997). “Experimental research on the determination of the main parameters affecting the behavior of reinforced concrete columns under fire conditions.” *Magazine of Concrete Research*, 49(179), 117–127.

Ersoy, U., Suleiman, R. and Tankut, T. (1993). “Behavior of jacketed columns.” *ACI Structural Journal*, 90(3), 288-293.

Giménez, E., Adam, J.M., Ivorra, S., Moragues, J.J., and Calderón, P.A. (2009). “Full-scale testing of axially loaded RC columns strengthened by steel angles and strips.” *Advances in Structural Engineering*, 12(2), 169-181.

Han, C. G., Han, M. C., and Heo, Y. S. (2009) “Improvement of residual compressive strength and spalling resistance of high-strength RC columns subjected to fire.” *Construction and Building Materials*, 23(1), 107–116.

Han, L. H. (2001). “Fire performance of concrete filled steel tubular beam-columns.” *Journal of Constructional Steel Research*, 57(6), 697–711.

Han, L. H., Zheng, Y. Q., and Teng, J. G. (2006). “Fire resistance of RC and FRP-confined RC columns.” *Magazine of Concrete Research*, 58(8), 533–546.

Han, L. H., Yang, Y. F., Yang, H., and Huo, J. S. (2002). “Residual strength of concrete-filled RHS columns after exposure to the ISO-834 standard fire.” *Thin-Walled Structures*, 40(12), 991–1012.

Han, L. H., Zhao, X. Y., Yang, Y. F., and Feng, J. B. (2003). “Experimental study and calculation of fire resistance of concrete-filled hollow steel columns.” *Journal of Structural Engineering*, 129(3), 346–356.

Han, L. H., and Huo, J. S. (2003). “Concrete-filled hollow structural steel columns after exposure to ISO-834 fire standard.” *Journal of Structural Engineering*, 129(1), 68–78.

Han, L. H., Yang, Y. F., and Xu, L. (2003). “An experimental study and calculation on the fire resistance of concrete-filled SHS and RHS columns.” *Journal of Constructional Steel Research*, 59(4), 427–452.

Han, L. H., and Lin, X. K. (2004). “Tests on cyclic behavior of concrete-filled hollow structural steel columns after exposure to the ISO-834 standard fire.” *Journal of Structural Engineering*, 130(11), 1807–1809.

ISO. (1975). ‘‘Fire resistance test—elements of building construction.’’ *ISO 834*, Geneva.

Jau, W. C., and Huang, K. L. (2008). “A study of reinforced concrete corner columns after fire.” *Cement and Concrete Composites*, 30(7), 622–638.

Karter, M. J. (2012). “Fire loss in the united states during 2011.” Fire Analysis and Research Division, National Fire Protection Association, MA, USA.

Kodur, V. K. R., and Raut, N. K. (2009). “Design equation for predicting fire resistance of reinforced concrete columns.” *Structural Concrete*, 10(2), 73–86.

Kodur, V. K. R., Bisby, L. A., and Green, M. F. (2006). “Experimental evaluation of the fire behaviour of insulated fibre-reinforced-polymer-strengthened reinforced concrete columns.” *Fire Safety Journal*, 41(7), 547–557.

Kodur, V. K. R. (1999). ‘‘Performance-based fire resistance design of concrete-filled steel columns.’’ *Journal of Constructional Steel Research*, 51(1), 21–26.

Kodur, V. K. R. (1998). ‘‘Performance of high strength concrete-filled steel columns exposed to fire.’’ *Canadian Journal of Civil Engineering*, 25(6), 975–981.

Kodur, V. K. R., Cheng, F. P., Wang, T. C., and Sultan, M. A. (2003). “Effect of strength and fiber reinforcement on fire resistance of high-strength concrete columns.” *Journal of Structural Engineering*, 129(2), 253–259.

Kodur, V. K. R., Wang, T. C., and Cheng, F. P. (2004). “Predicting the fire resistance behaviour of high strength concrete columns.” *Cement and Concrete Composites*, 26(2), 141–153.

Lie, T. T. (1992). “ASCE Manuals and Reports on Engineering Practice No. 78-Structural Fire Protection.” American Society of Civil Engineers, New York.

Lie, T. T., and Kodur, V. K. R. (1996). “Fire resistance of steel columns filled with bar-reinforced concrete.” *Journal of structural engineering New York*, 122(1), 30–36.

Lin, C. H., Chen, S. T., and Yang, C. A. (1995). “Repair of fire-damaged reinforced concrete columns.” *ACI Materials Journal*, 92(4), 406–411.

Raut, N. K., and Kodur, V. K. R. (2011). “Response of high-strength concrete columns under design fire exposure.” *Journal of Structural Engineering*, 137(1), 69–79.

Su, R.K.L., Cheng, B., Wang, L., Siu, W.H. and Zhu, Y. (2011). “Use of bolted steel plates for strengthening of reinforced concrete beams and columns”, *The IES Journal Part A: Civil & Structural Engineering*, 4(2), 55-68.

Su, R.K.L., Siu, W.H. and Smith, S.T. (2010). “Effects of bolt-plate arrangements on steel plate strengthened reinforced concrete beams.” *Engineering Structures*, 32(6), 1769-1778.

449 Su, R.K.L., and Wang, L. (2012). “Axial strengthening of preloaded rectangular concrete columns by
450 precambered steel plates.” *Engineering Structures*, 38(5), 42-52.

451 Takeuti, R.A., de Hanai, J.B. and Mirmiran, A. (2008). “Preloaded RC columns strengthened with
452 high-strength concrete jackets under uniaxial compression.” *Materials and Structures*, 41(7),
453 1251-1262.

454 Tan, K. H., and Yao, Y. (2003). “Fire Resistance of Four-Face Heated Reinforced Concrete Columns.”
455 *Journal of Structural Engineering*, 129(9), 1220–1229.

456 Tao, Z., Wang, Z. B., Han, L. H., and Brian, B. (2011) “Fire performance of concrete-filled steel
457 tubular columns strengthened by CFRP.” *Steel and Composite Structures*, 11(4), 307–324.

458 Tao, Z., and Han, L. H. (2007) “Behaviour of fire-exposed concrete-filled steel tubular beam columns
459 repaired with CFRP wraps.” *Thin-Walled Structures*, 45(1), 63–76.

460 Tao, Z., Han, L. H., and Wang, L. L. (2007) “Compressive and flexural behaviour of CFRP-repaired
461 concrete-filled steel tubes after exposure to fire.” *Journal of Constructional Steel Research*, 63(8),
462 1116–1126.

463 Wang, L. and Su, R.K.L. (2012a). “Experimental investigation of preloaded RC columns strengthened
464 with precambered steel plates under eccentric compression loading.” *Advances in Structural*
465 *Engineering*, (Article in press).

466 Wang, L. and Su, R.K.L. (2012b). “Theoretical and experimental study of plate-strengthened concrete
467 columns under eccentric compression loading.” *Journal of Structural Engineering*, (Article in
468 press).

469 Wu, B., Hong, Z., Tang, G. H., and Wang, C. (2007). “Fire resistance of reinforced concrete columns
470 with square cross section.” *Advances in Structural Engineering*, 10(4), 353–369.

471 Wu, B., and Xu, Y. Y. (2009). “Behavior of axially-and-rotationally restrained concrete columns with
472 '+'-shaped cross section and subjected to fire.” *Fire Safety Journal*, 44(2), 212–218.

473 Xu, Y. Y., and Wu, B. (2009). “Fire resistance of reinforced concrete columns with L-, T-, and +-
474 shaped cross-sections.” *Fire Safety Journal*, 44(6), 869–880.

Yaqub, M., and Bailey, C. G. (2011). "Fire resistance of steel columns filled with bar-reinforced concrete." *Construction and Building Materials*, 25 (1), 359–370.

Table 1. Summary of the material and geometry properties for repair works

Specimen	$f_{cu,s}$ (MPa)	$f_{c,s}'$ (MPa)	$f_{cu,t}$ (MPa)	$f_{c,t}'$ (MPa)	L_{rc} (mm)	t (min)	t_p (mm)	δ (mm)	P_{pl} (kN)
FSC1	53.2	48.3	54.1	48.8	850	-	-	-	-
FSC2	53.2	48.3	54.1	48.8	850	240	-	-	-
FSC3	52.4	46.5	52.8	46.7	850	240	8	10	640
FSC4	52.4	46.5	52.8	46.7	850	240	6	10	830
FSC5	54.2	47.8	54.7	47.8	850	240	6	6	640
FSC6	54.2	47.8	54.7	47.8	850	240	6	10	640
FSC7	54.9	46.3	54.9	46.3	850	240	6	14	640

Note: $f_{cu,s}$ is the concrete cube compression strength on the 28th day;
$f_{c,s}'$ is the concrete cylinder compression strength on the 28th day;
$f_{cu,t}$ is the concrete cube compression strength on the fire test day;
$f_{c,t}'$ is the concrete cylinder compression strength on the fire test day.

Table 2. Material properties of reinforcements and steel plates

Steel Plate		
Thickness	f_{yp} (MPa)	E_p (GPa)
6 mm	329	209
8 mm	322	195

Reinforcement bars		
Specimen	f_y (MPa)	E_s (GPa)
T12	516	198
T16	507	196
R6	464	186
R8	437	187

Table 3. Summary of deformability and ductility factors, axial load capacities and predicted values

Specimen	Δ_y (mm)	Δ_u (mm)	Δ_f (mm)	λ	η	P_{exp} (kN)	P_{pre} (kN)	P_{exp} / P_{pre}
FSC1	2.55	2.77	3.11	1.12	1.09	3085	3020	1.02
FSC2	4.77	6.75	8.03	1.19	1.42	1280	1012	1.26
FSC3	3.53	7.79	13.41	1.73	2.21	2227	1911	1.17
FSC4	2.77	5.85	9.13	1.56	2.11	1686	1479	1.14
FSC5	5.22	6.99	9.36	1.34	1.73	1522	1490	1.02
FSC6	3.48	7.27	11.28	1.55	2.09	1950	1738	1.12
FSC7	3.39	7.13	10.78	1.51	2.10	2153	1913	1.13
Mean	-	-	-	-	-	-	-	1.12

Table 4. Internal load distributions of strengthened columns

Section	FSC3						FSC4					
	Post-stress		75% P_{exp}		P_{exp}		Post-stress		75% P_{exp}		P_{exp}	
	P_{pc}	P_{rc}	P_{pc}	P_{rc}	P_{pc}	P_{rc}	P_{pc}	P_{rc}	P_{pc}	P_{rc}	P_{pc}	P_{rc}
1	388	252	977	693	1305	922	363	467	593	672	743	943
2	379	261	966	704	1313	914	361	469	608	657	720	966
3	411	229	1021	649	1332	895	344	486	577	688	659	1027
4	404	236	973	697	1321	906	381	449	584	681	707	979
	FSC5						FSC6					
1	296	344	616	524	845	675	336	274	766	697	955	995
2	271	369	617	523	864	656	361	279	779	684	964	986
3	324	316	637	503	922	598	344	296	797	666	1015	935
4	311	329	661	479	915	605	342	298	811	652	1022	928
	FSC7											
1	380	260	867	747	1185	968	Note: P_{pc} is the axial compressive load of steel plates in kN; P_{rc} is the axial compressive load of RC column in kN.					
2	389	251	956	658	1233	920						
3	412	228	871	743	1262	891						
4	344	296	913	701	1201	952						

A List of Figure Captions

Figure 1. The specimen configuration: (a) Elevation; (b) Cross section

Figure 2. Test setup: (a) Photograph of the furnace; (b) Photograph of the compression machine

Figure 3. Positions of the thermocouples in the concrete

Figure 4. Measured furnace temperature (*T*) versus time (*t*)

Figure 5. Instrumentation of Specimen FSC6

Figure 6. Crack and spalls of specimens after the fire test

Figure 7. Post-stressed procedure (a) Cement mortar repairing of FSC5 and (b) Injection plaster filled in the gaps

Figure 8. Post-stressed procedure (a) Schematic diagram, (b) The Steps (i) to (iii) of FSC6 and (c) Strengthening details of FSC6

Figure 9. Concrete temperature versus time: (a) Section B-B of FSC4; (b) Section B-B of FSC7; (c) 70 mm from the surface of FSC2; (d) 125 mm from the surface of FSC5

510 Figure 10. Axial compression-shortening curves of the specimens: (a) Effects of fire exposure; (b)
511 Effects of plate thickness; (c) Effects of initial precamber; (d) Effects of preloading level
512 Figure 11. Crack patterns and failure mode
513 Figure 12. Repaired columns fire protected by gypsum wallboard
514

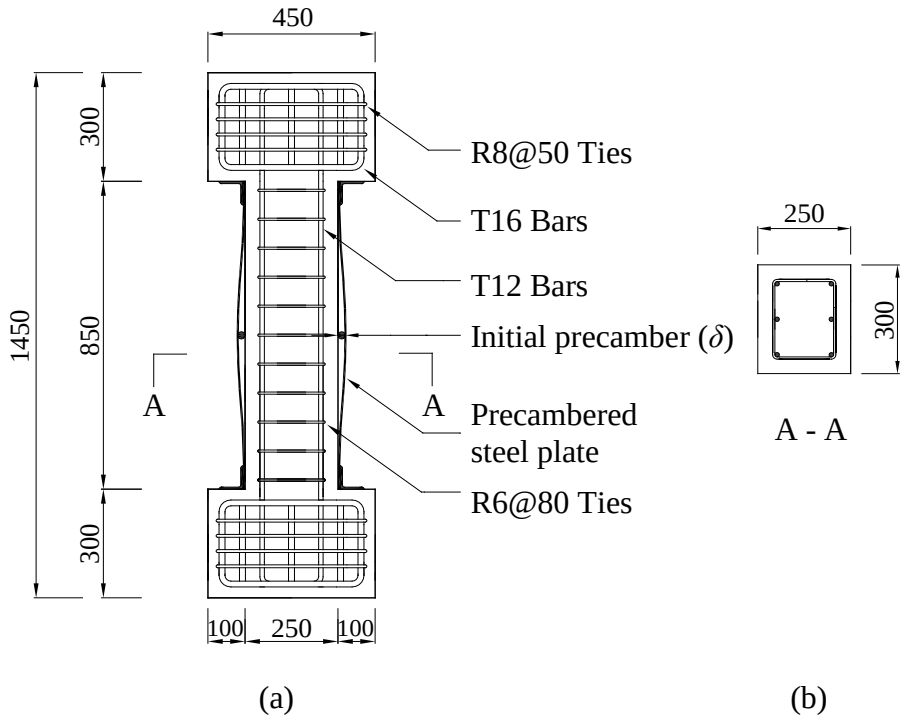

Fig. 1. The specimen configuration: (a) Elevation; (b) Cross section

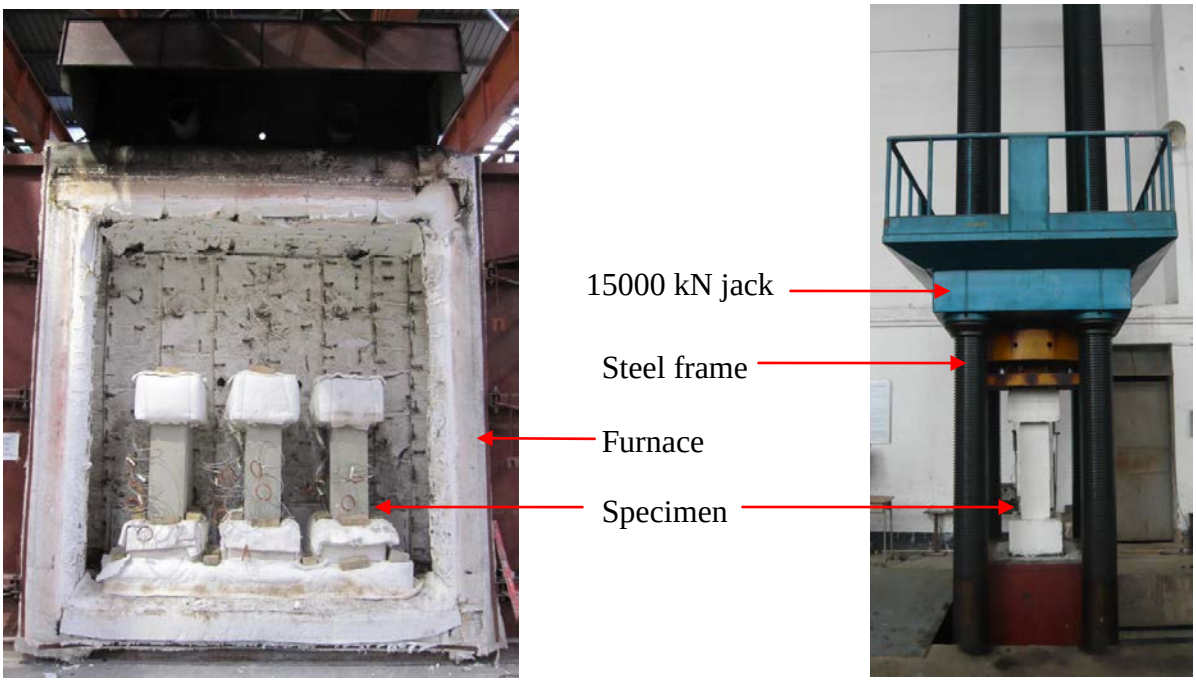

Fig. 2. Test setup: (a) Photograph of the furnace; (b) Photograph of the compression machine

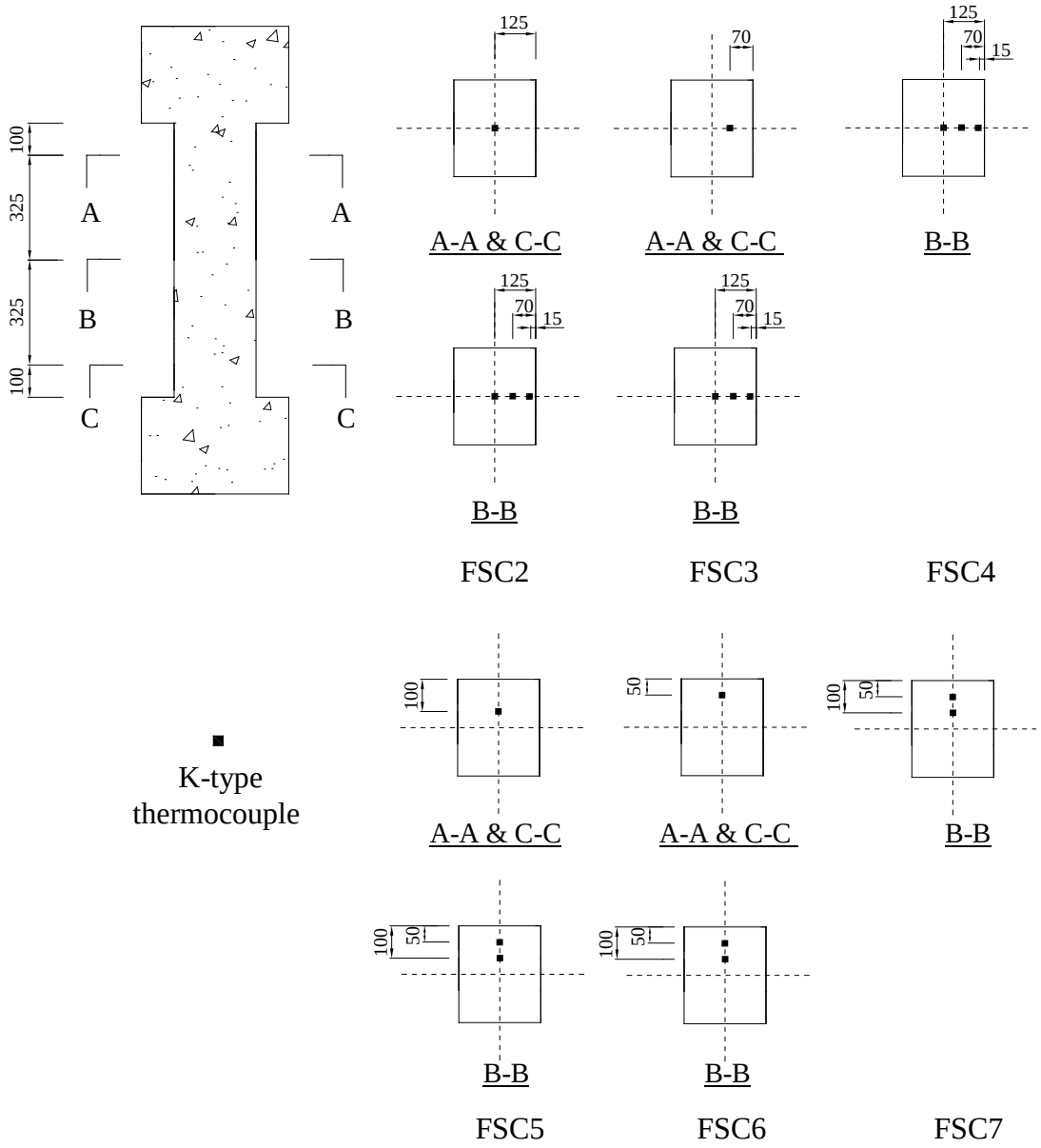

Fig. 3. Positions of the thermocouples in the concrete

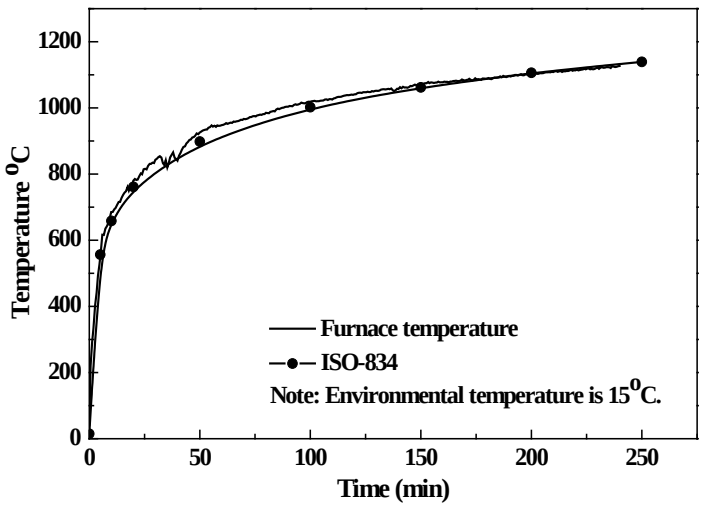

Fig. 4. Measured furnace temperature (T) versus time (t)

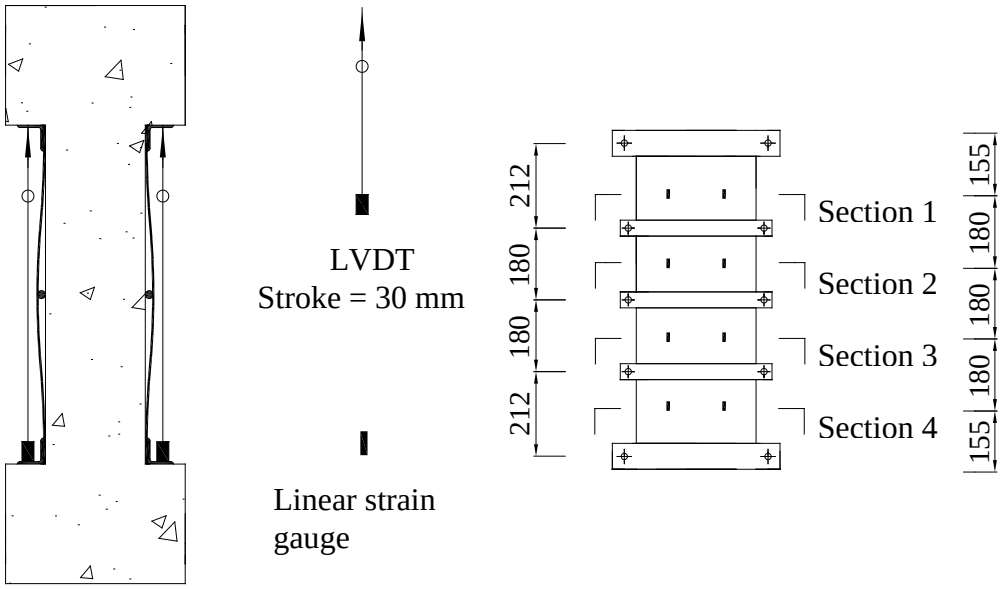

Fig. 5. Instrumentation of Specimen FSC6

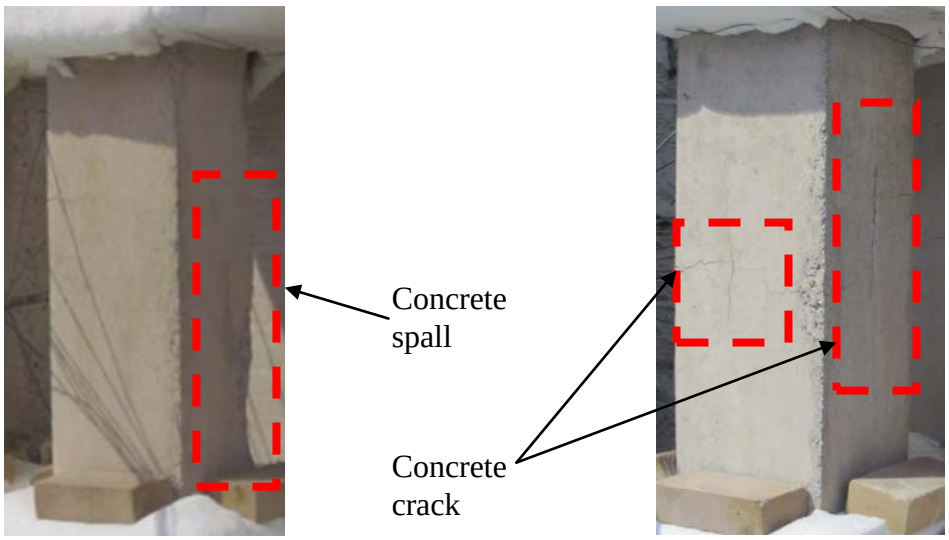

Fig. 6. Crack and spalls of specimens after the fire test

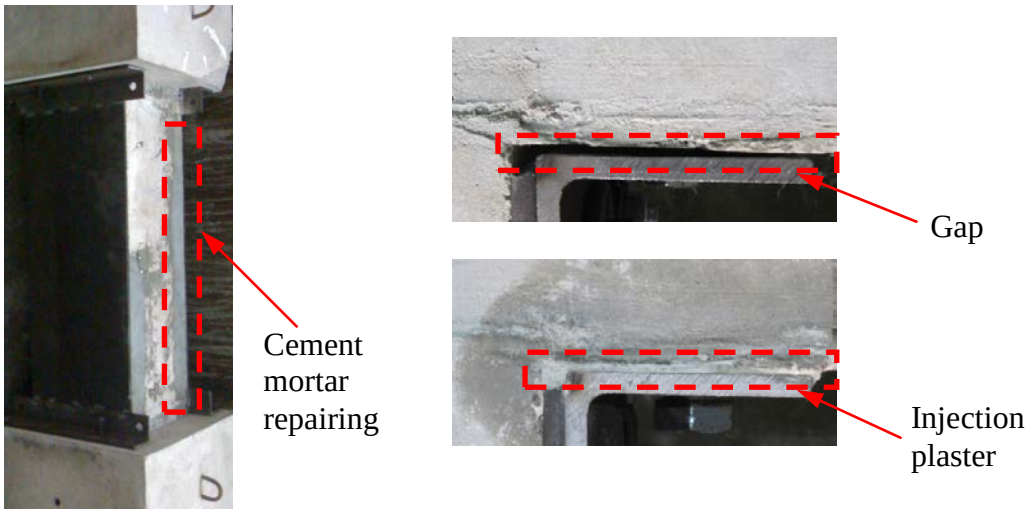

Fig. 7. Post-stressed procedure (a) Cement mortar repairing of FSC5 and (b) Injection plaster filled in the gaps

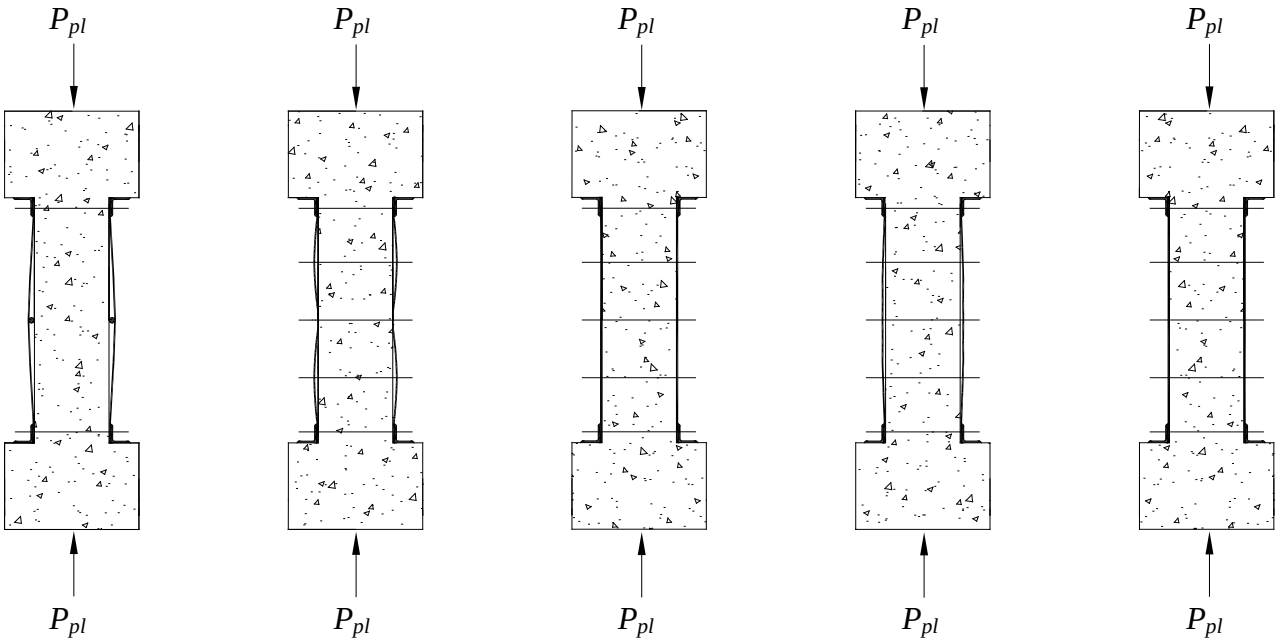

(i) Initial state | (ii) Tightening the mid-height bolts | (iii) Flattening the plates | (iv) Loosening the bolts | (v) Fastening the bolts again

(a)

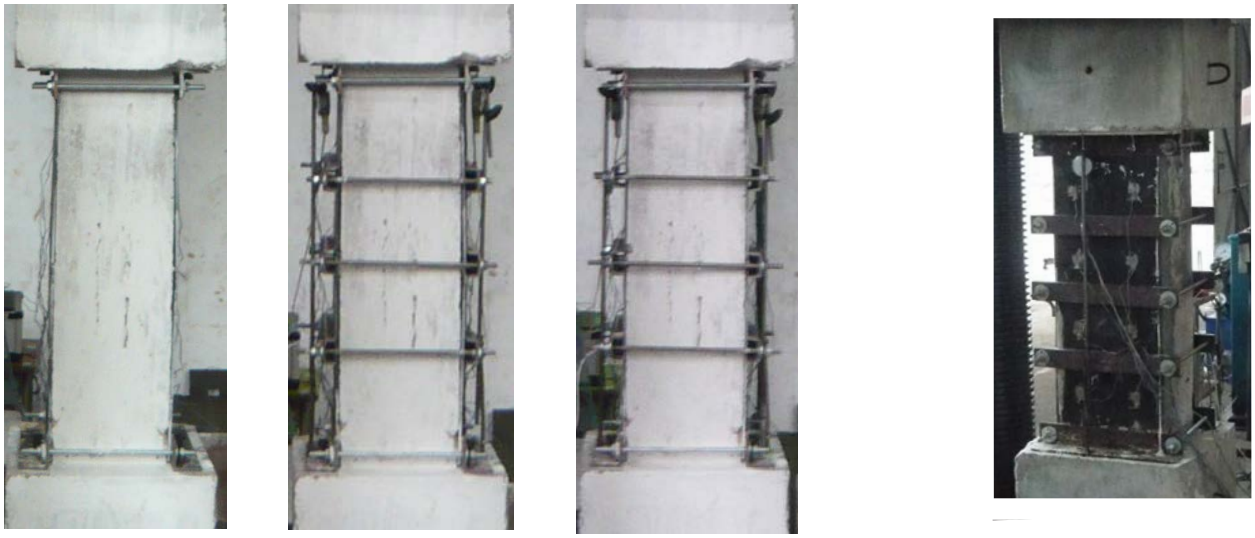

(b) (c)

Fig. 8. Post-stressed procedure (a) Schematic diagram, (b) The Steps (i) to (iii) of FSC6 and (c) Strengthening details of FSC6

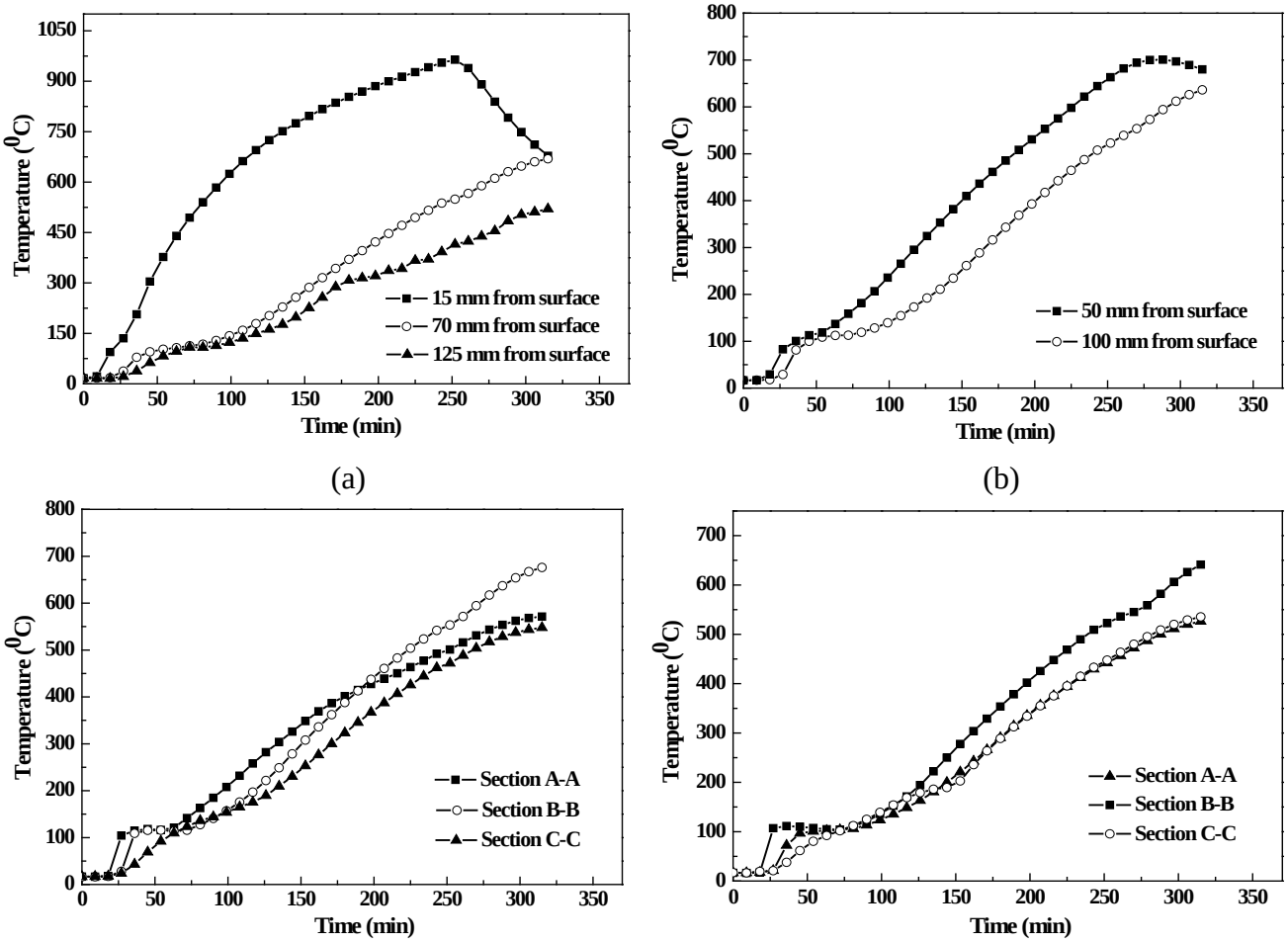

Fig. 9. Concrete temperature versus time: (a) Section B-B of FSC4; (b) Section B-B of FSC7; (c) 70 mm from the surface of FSC2; (d) 125 mm from the surface of FSC5

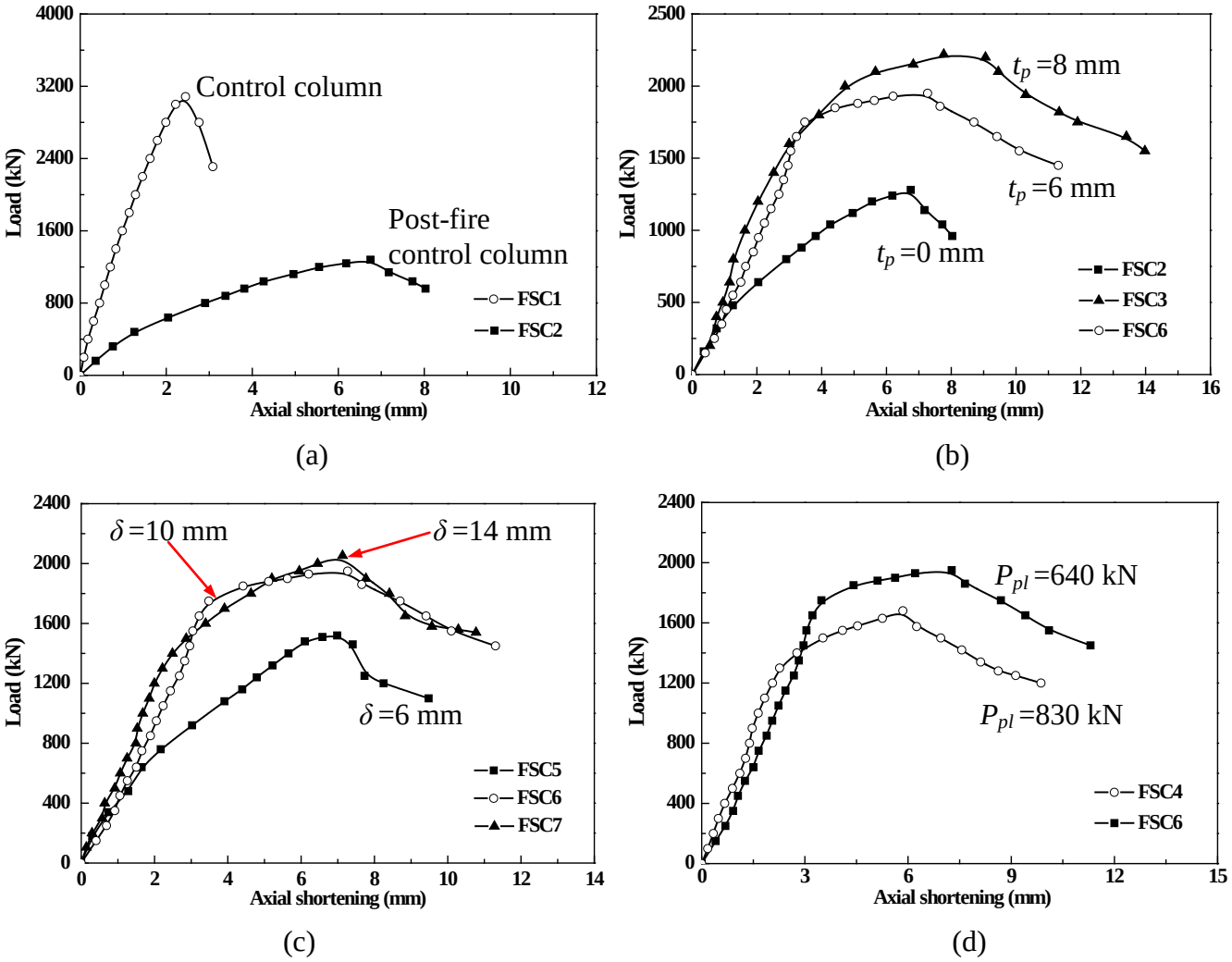

Fig. 10. Axial compression-shortening curves of specimens: (a) Effects of fire exposure; (b) Effects of plate thickness; (c) Effects of initial precamber; (d) Effects of preloading level

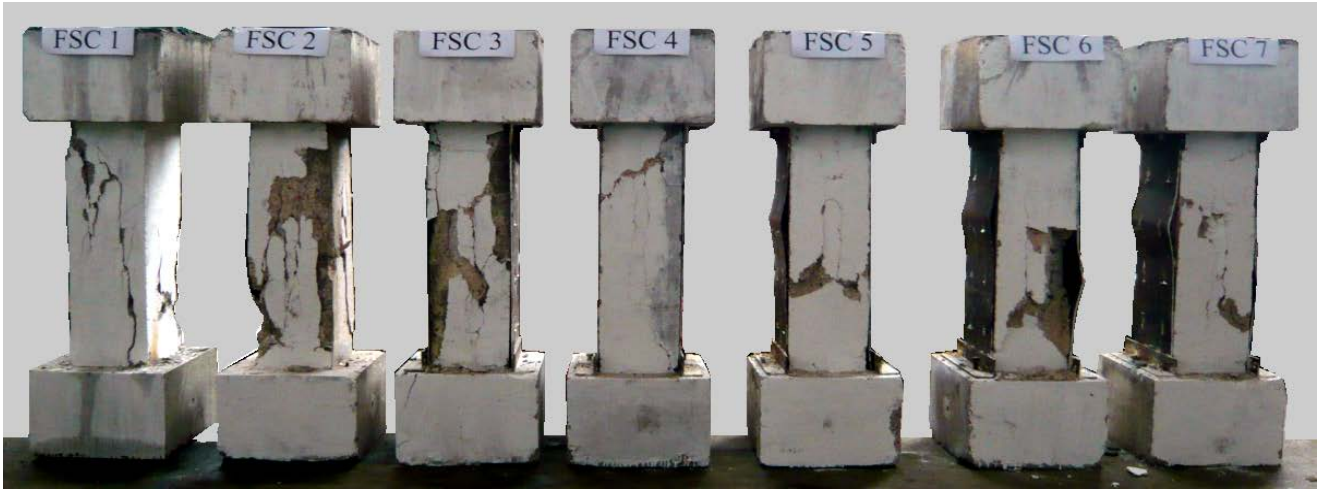

Fig. 11. Crack patterns and failure mode

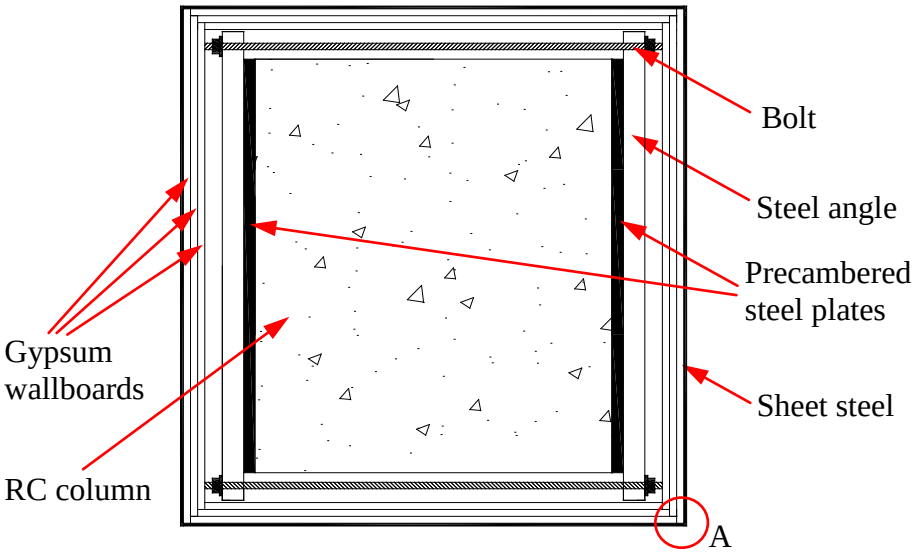

Note: The corner joint details (A) are shown in ASCE/SEI/SFPE 2007.

Fig. 12. Repaired columns fire protected by gypsum wallboard